



LAWRENCE
LIVERMORE
NATIONAL
LABORATORY

Speckle lifetime in high-contrast adaptive optics

B. Macintosh, L. Poyneer, A. Sivaramakrishnan,
C. Marois

August 22, 2005

SPIE Conference on Astronomical Adaptive Optics Systems
and Applications II
San Diego, CA, United States
July 31, 2005 through August 4, 2005

Disclaimer

This document was prepared as an account of work sponsored by an agency of the United States Government. Neither the United States Government nor the University of California nor any of their employees, makes any warranty, express or implied, or assumes any legal liability or responsibility for the accuracy, completeness, or usefulness of any information, apparatus, product, or process disclosed, or represents that its use would not infringe privately owned rights. Reference herein to any specific commercial product, process, or service by trade name, trademark, manufacturer, or otherwise, does not necessarily constitute or imply its endorsement, recommendation, or favoring by the United States Government or the University of California. The views and opinions of authors expressed herein do not necessarily state or reflect those of the United States Government or the University of California, and shall not be used for advertising or product endorsement purposes.

Speckle lifetimes in high-contrast adaptive optics

Bruce Macintosh^{*ab}, Lisa Poyneer^{ab}, Anand Sivaramakrishnan^{acd}, Christian Marois^{ab}

^aNSF Center for Adaptive Optics

^bLawrence Livermore National Laboratory, 7000 East Ave., Livermore, CA 94551

^cSpace Telescope Science Institute, 3700 San Martin Drive, Baltimore, MD 21218

^dAstrophysics Department, The American Museum of Natural History, 79th Street at Central Park West, New York, NY 10024-5192

ABSTRACT

The main noise source in detection of faint companions such as extrasolar planets near bright stars with AO is speckle noise - residual PSF structure caused by wavefront errors due to the atmosphere, the AO system, and static optical effects. Of these, the most fundamental are atmospheric speckles - even given infinite wavefront SNR and a perfect DM, timelag between sensing and correction will always lead to a residual atmospheric speckle pattern. There have been several suggestions as to the lifetime of these atmospheric speckles, none strongly supported by theory or simulation. We have carried out a systematic series of simulations and analysis to explore this question. We show that speckles have different behavior in the regime in which diffraction is significant (first-order speckles, which are rapidly modulated as a phase error translates across the aperture) and in the coronagraphic regime (second-order speckles, which evolve only as the phase screen completely clears the aperture.). We use simulations to analyze the behavior of speckles in a variety of regimes, showing that the second-order atmospheric speckle lifetime is almost constant irrespective of the properties of the AO system, and is set primarily by the atmospheric clearing time of the telescope aperture.

Keywords: Adaptive optics, extrasolar planets, speckle, coronagraphs

1. INTRODUCTION

Ground-based adaptive optics (AO) imaging is always imperfect. Even in an ideal AO system there will be wavefront errors caused by noise in the individual wavefront measurements (measurement noise), by the inability of the system to measure and reproduce all spatial frequencies present in the atmosphere (fitting error), and by the finite temporal bandwidth of the AO loop (bandwidth error i.e. the delay between measurement and correction.) As a result, images of stars are surrounded by a pattern of scattered light, limiting our ability to see faint companions to bright stars. If the only deviations from smoothness in this halo were caused by the Poisson noise of the halo photons themselves, it would be possible with even a modest AO system to successfully detect companions 10^9 or more dimmer than their parent star with moderate (hour-long) integrations, at least for sufficiently bright stars. However, the halo is not smooth. Instantaneously it is broken up into an interference pattern of bright speckles, each comparable in size and shape to a true companion; this speckle noise is the most fundamental limitation in detection of faint companions.¹

In addition to random processes, non-random errors such as mis-calibrations of the adaptive optics system or imperfections in optics (e.g. errors on the telescope primary mirror that the AO system cannot correct) will produce long-lived speckles that evolve only when processes such as flexure produce optical changes in the system. Although these quasi-static speckles produce a significant noise floor in moderate exposure times in most current AO systems, they can in principal be removed by imaging techniques such as comparing a series of images at different orientations² or by precision calibration of the adaptive optics system³. We will not treat such quasi-static speckles in this paper but instead examine the fundamental limit of speckles caused by atmospheric and measurement wavefront error sources.

To the extent that these speckles are caused by random processes, with a sufficiently long exposure time multiple realizations of the speckle pattern will produce a smooth PSF. The key question is the timescale on which this smoothing occurs, which we will refer to as the speckle lifetime. In simulation, this can be evaluated by comparing the

* bmac@igpp.llnl.gov

variance of the intensity of the point spread function p at a given location in a series of exposures of a given exposure time t_{int} . For a random process, we would expect this variance to decrease as $\text{var}[p] \propto \frac{t_{dec}}{t_{int}}$ for $t_{int} > t_{dec}$.

Different authors have made several suggestions for this decorrelation timescale. Angel⁴ assumed that the speckle pattern changes completely with each update of the AO system – $t_{dec} = \Delta t$. Racine¹ after Roddier⁵ takes the speckle lifetime to be the Fried parameter r_0 divided by the dispersion in the wind velocity across multiple layers Δv . However, the Roddier paper dealt with open-loop (non-AO) images for applications such as speckle interferometry, where low-order aberrations such as tip-tilt can significantly impact the speckle lifetime; the results, as shown below, do not apply to the high Strehl ratio case. Olivier et al.⁶ show simulations that give a much longer speckle lifetime; for a telescope diameter D and a wind speed v , they find a speckle lifetime of $0.4D/v$ irrespective of r_0 . Other authors have suggested that the speckle lifetime is dependent on position in the field. To resolve this question, we have carried out a series of numerical simulations and simple analytic calculations.

2. FIRST AND SECOND ORDER SPECKLE LIFETIMES

We express the electric field in the pupil plane of an AO-corrected telescope as $E(\mathbf{x}) = A(\mathbf{x})e^{i\phi(\mathbf{x})}$ where $\mathbf{x}=(x,y)$ is a coordinate vector in the pupil plane. The resulting point spread function (PSF) can be expressed as a Taylor series expansion of the Fourier transform of this quantity squared; in the high Strehl regime this reduces to^{7,8}

$$\begin{aligned} p(\mathbf{k}) &\cong p_0 + p_1 + p_2 \\ &= aa^* \\ &\quad - i[a(a^* * \Phi^*) - a^*(a * \Phi)] \\ &\quad + (a * \Phi)(a^* * \Phi^*) - \frac{1}{2}[a(a^* * \Phi^* * \Phi^*) + a^*(a * \Phi * \Phi)] \end{aligned}$$

where a and Φ are the Fourier transforms of A and ϕ respectively, $*$ denotes convolution, and $\mathbf{k}=2\pi(\theta_x, \theta_y)/\lambda$ is the spatial frequency corresponding to a given position in the focal plane. The zero-order term is the classic diffraction pattern; the first order term is the ‘‘pinned speckle’’ term which modulates the Airy pattern⁹, and the second order term is a combination of the fundamental PSF halo ($a^* \Phi)(a^* * \Phi^*)$ with an additional ‘‘Strehl’’ term that serves to remove light from the PSF core. The diffraction pattern and the pinned speckle term dominate at moderate angles for normal AO systems/cameras but can be suppressed by any one of a variety of coronagraphs; a mathematically simple though physically impractical example is apodizing the aperture function with a smoothly-varying $A(\mathbf{x})$ so that $a(\mathbf{k})$ drops rapidly to zero for large \mathbf{k} . In a coronagraphic system, once diffraction has been suppressed, the PSF halo term – essentially the power spectrum of the input phase aberration – is the primary source of scattered light. (When the second-order term is very small due to high-accuracy wavefront control a fourth-order term becomes significant at some radii¹⁰, but this generally does not apply in the adaptive optics regime.) Figure 1 illustrates this concept, showing an input phase error and its PSF for two pupils, a hard-edged telescope aperture and an apodized coronagraph.

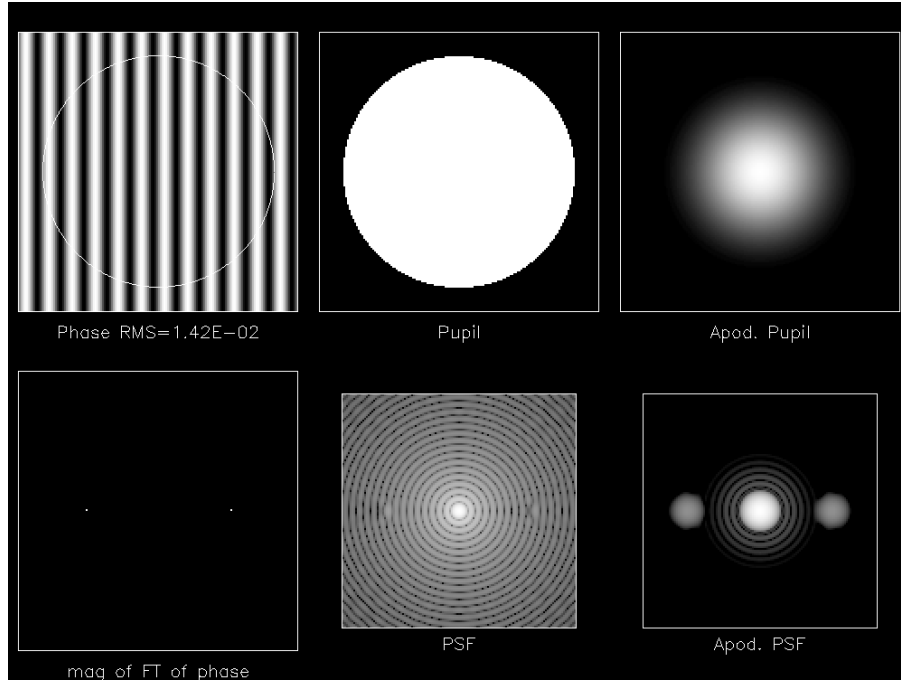


Figure 1: Illustration of the PSF of a coronagraphic and non-coronagraphic system. Upper left: input phase aberration. Upper center: pupil function A for a normal telescope. Lower center: corresponding PSF showing an antisymmetric pair of pinned speckles. Upper right: apodized A . Lower right: corresponding PSF showing a symmetric pair of halo speckles.

If we consider a sinusoidal phase aberration, $\phi(\mathbf{x}) = \varepsilon \cos(\mathbf{k}_0 \cdot (\mathbf{x} - \mathbf{x}_0))$ its Fourier transform can be written as

$$\Phi(\mathbf{k}) = \frac{1}{2} \varepsilon (e^{-i\mathbf{k} \cdot \mathbf{x}_0} \delta(\mathbf{k} - \mathbf{k}_0) + e^{i\mathbf{k} \cdot \mathbf{x}_0} \delta(\mathbf{k} + \mathbf{k}_0))$$

Taking advantage of the fact that a is real and symmetric, we can write the first order speckle term as

$$p_1(\mathbf{k}) = \varepsilon a(\mathbf{k})(a(\mathbf{k} - \mathbf{k}_0) - a(\mathbf{k} + \mathbf{k}_0)) \sin(\mathbf{k}_0 \cdot \mathbf{x}_0)$$

This describes an antisymmetric pair of pinned speckles, located at positions $\pm \mathbf{k}\lambda/2\pi$. If the phase ripple is moving across the telescope with some wind velocity \mathbf{v} so that $\mathbf{x}_0 = \mathbf{v}t$, this becomes

$$p_1(\mathbf{k}) = \varepsilon a(\mathbf{k})(a(\mathbf{k} - \mathbf{k}_0) - a(\mathbf{k} + \mathbf{k}_0)) \sin(\mathbf{k}_0 \cdot \mathbf{v}t)$$

The pinned speckles will be modulated with a period $\mathbf{k}_0 \cdot \mathbf{v}$. By contrast, the second order PSF term for this aberration is simply the power spectrum of $\phi(\mathbf{x}) = \varepsilon \cos(\mathbf{k}_0 \cdot (\mathbf{x} - \mathbf{x}_0))$, which is independent of \mathbf{x}_0 , and hence does not evolve with time.

An arbitrary phase aberration can of course be decomposed into individual sinusoidal phase ripples, each of which will behave as above, with a location in the PSF. As a result, if a fixed phase screen is translated across the telescope aperture, at a given location in the PSF $\boldsymbol{\theta}$ corresponding to a frequency $\mathbf{k} = 2\pi\boldsymbol{\theta}/\lambda$ the first-order speckles will all modulate with periods $2\pi\boldsymbol{\theta} \cdot \mathbf{v}/\lambda$. If diffraction has been suppressed, by contrast, the speckles will be steady and only evolve as new realizations of the atmosphere transit the telescope. We carried out simulations with a frozen atmospheric screen, with low spatial frequencies filtered to approximate a conventional AO system, to study these two separate behaviors. Figure 2, Figure 3, and Figure 4 illustrate the strong modulation of the first-order speckles in an unapodized system contrasted with the slow evolution of an apodized (coronagraphic) system.

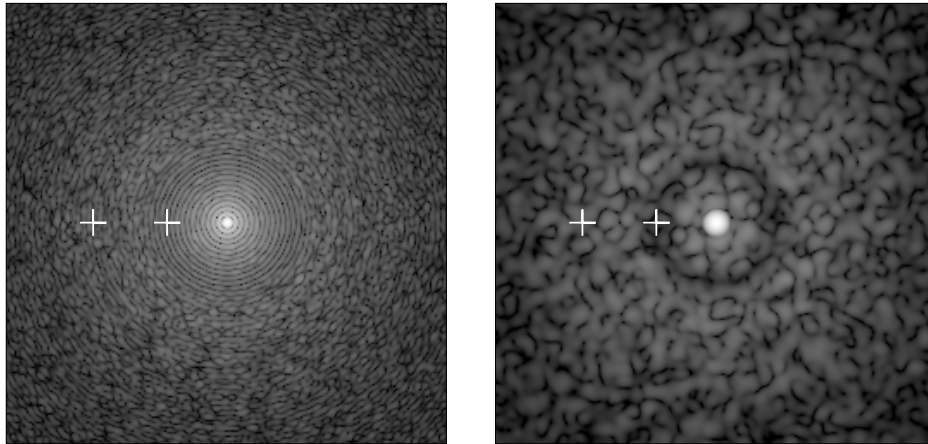


Figure 2: Representative PSFs in a unapodized (left) and apodized (right) system, from a simple AO simulation. Wind is blowing left to right. The crosses indicate the locations where the timeseries in Figure 3 and Figure 4

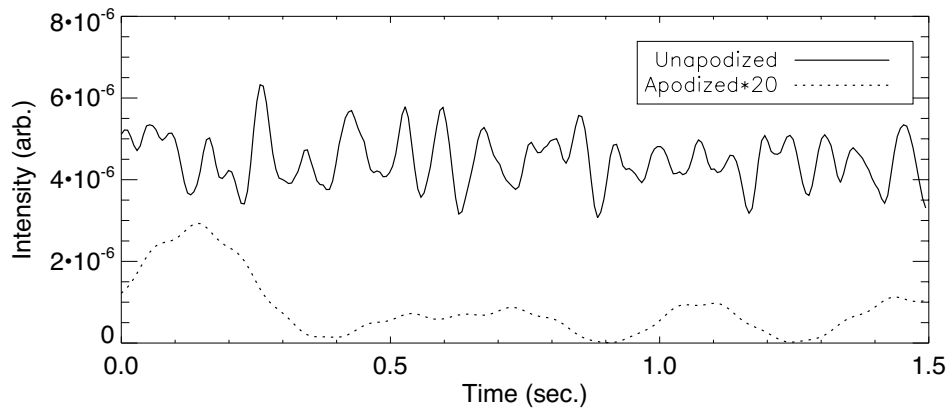


Figure 3: Timeseries of the PSF intensity at $11 \lambda/D$ radius in the upwind direction for both the apodized and unapodized PSFs.

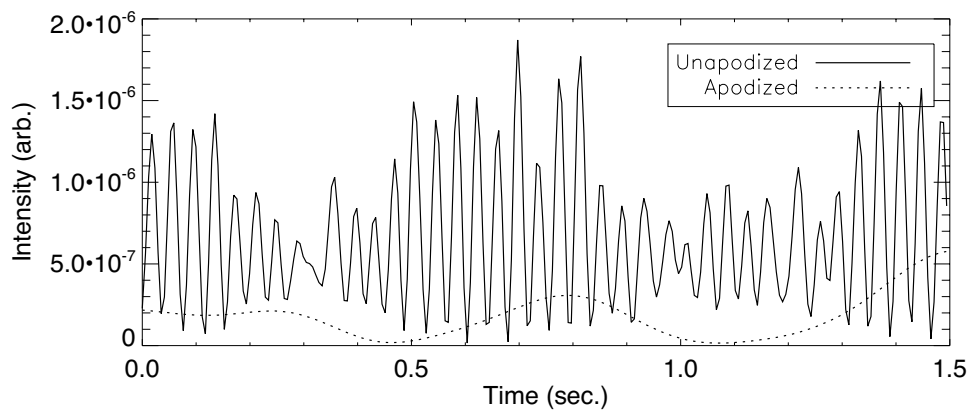


Figure 4: Timeseries of the PSF intensity at $26 \lambda/D$ radius.

3. FULL AO SIMULATIONS

High-contrast imaging systems will almost by definition incorporate some class of coronagraph, so for the remainder of this paper we will use an apodized pupil for all simulations and consider only the evolution of the second-order speckle terms.

To fully evaluate the speckle lifetime we used a closed-loop AO simulation of a extreme AO system similar to the proposed Extreme Adaptive Optics Coronagraph (ExAOC) for the Gemini Observatory. The parameters of the simulation are given below.

Telescope diameter D	8.0 m
Subaperture size d	0.18 m
AO system time step Δt	1/1500 Hz
Wavefront sensor type	Spatially-filtered Shack-Hartmann ¹¹
Controller lag	2 time steps
r_0 @ 500 nm	One layer 0.18 m
Wind velocity	10 m/s
Science wavelength	1.65 μm
Target star brightness	$I=7$ mag
Coronagraph	Blackman-apodized pupil

Table 1: Simulation parameters.

The simulation was run for integration times up to 20 seconds to produce science-camera PSF movie cubes $p(\theta, t)$ at 100 Hz rate. A typical long-exposure PSF is shown in Figure 5. The square dark hole of size $\lambda/d=1.8$ arcseconds is produced where the AO system has removed most wavefront errors over a range of spatial frequencies. The wind is blowing from top to bottom; different regions within the dark hole are dominated by temporal bandwidth errors (the butterfly pattern) and WFS measurement noise (filling in the remainder of the dark hole.) The PSF outside the dark hole is dominated by atmospheric fitting error and essentially unmodified by the AO system, which cannot measure or correct the corresponding spatial frequencies. By studying different regions in these PSFs we can compare the evolution of speckles caused by different wavefront error sources. The simulation was run in three cases: atmosphere-only, wavefront sensor noise only, and with both error sources present.

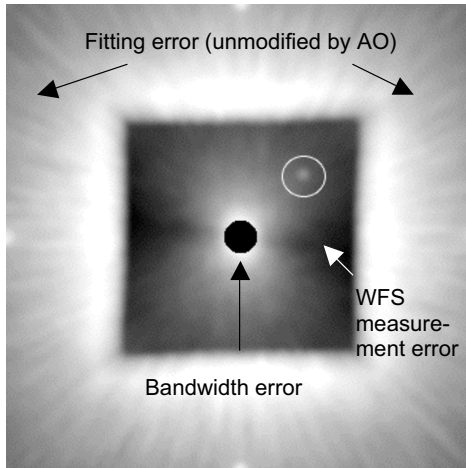


Figure 5: Simulated ExAO system PSF. Different regions of the PSF are dominated by speckles caused by different error sources, as indicated.

The speckle variance was evaluated at each point in the PSF for successively longer integration times using a temporal power spectrum technique. The speckle decorrelation time t_{dec} is defined as the time for the variance to drop to half its short-exposure value.

4. DISCUSSION OF THE RESULTS

4.1 Single-layer atmosphere only

Figure 6 shows the speckle variance for several field points, located both within the dark hole, where speckles are due primarily to the finite temporal bandwidth of the AO system, and outside the dark hole, where speckles are caused purely by atmospheric fitting error. The speckle lifetime is essentially the same in both regions – the AO system has no effect on the decorrelation of speckles.

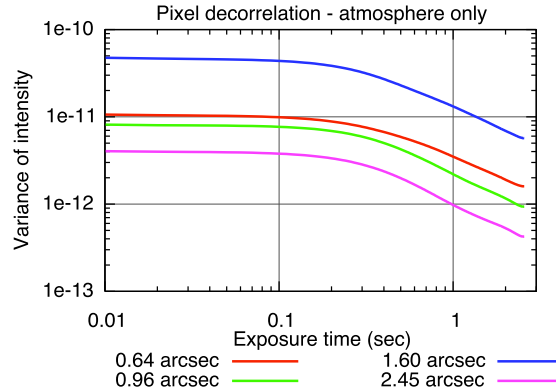


Figure 6: Speckle variance as a function of exposure time for several field locations in a case with no WFS measurement noise.

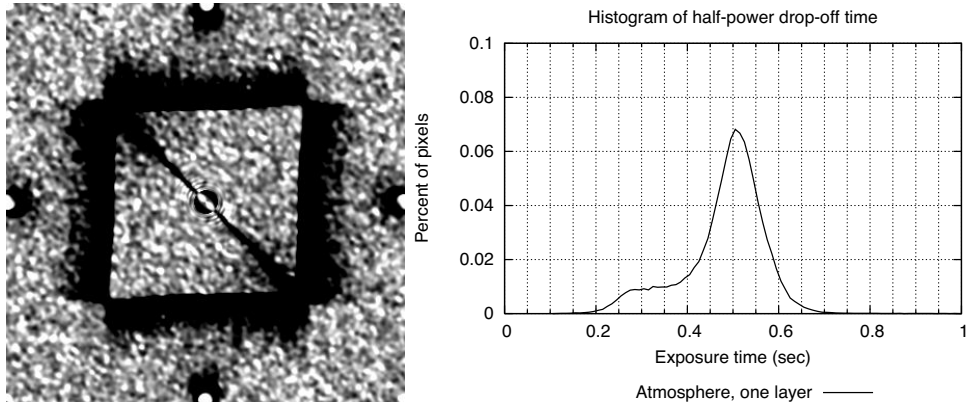


Figure 7: Left: Map of speckle lifetimes across the PSF; black indicates short-lived speckles while white indicates long-lived speckles. Single wind layer blowing at a 45 degree angle from the top right to bottom left. Right: histogram of speckle lifetimes.

Figure 7 shows this more clearly. The speckle lifetime was evaluated at each point in the PSF. Except for a narrow region surrounding the dark hole, where the deformable mirror influence function is injecting extra high-frequency noise, the speckle lifetime is unmodified by the AO system. The histogram shows that the median speckle lifetime for atmosphere errors is $t_{dec,atmos}=0.6D/v$. Note that the constant 0.6 is somewhat dependent on the coronagraph used – our Blackman apodization window decreases the effective aperture and hence decreases the speckle lifetime. We will evaluate the speckle lifetime for other coronagraphs in future work. Changing r_0 has no effect on this, since it merely scales the magnitude of the phase screens without changing their spatial or temporal properties.

4.2 Mixed bandwidth and measurement noise

Simulations show that speckles caused only by measurement noise decorrelate very rapidly, with $t_{\text{dec,meas}} \propto \Delta t$ where Δt is the update rate of the AO system. The exact constant of proportionality depends on the details of the controller and will be investigated in a future paper; for a simple controller it is on the order of 1/10.

The PSF formalism shown in section 3 shows that in a long-exposure image the average PSF halo intensity is the spatial power spectrum of the wavefront errors. If multiple independent error sources are present, the total power spectrum will be the sum of the individual power spectra of each error source; as a result, the PSF halo will be the sum of the PSF halo that would be produced by each individual error source in isolation. Since each error source has its own speckle lifetime, we expected that the PSF variance would also be the sum of the individual variances. For example, in regions where both measurement and bandwidth errors are significant, the speckle variance would be given rapidly decrease as the measurement-error speckles decorrelate and reach a plateau set by atmospheric errors until $t_{\text{int}} > t_{\text{dec,atmos}}$. Our simulations show that this is roughly the case, but especially $t_{\text{int}} = t_{\text{dec,atmos}}$ the total variance is somewhat greater than the sum of the variances of the two individual noise sources. This is due to cross-correlation terms in the PSF expansion between the two error sources, even when they are independent, and will be explored in a future paper. Still, at long exposure times the long-lived atmospheric speckles generally dominate. Simulations in Stahl and Sandler¹² appear to show that a quasi-predictive controller changed the speckle lifetime, but we believe that it merely decreased the total power in the atmospheric speckles (equivalent to lowering the solid curve in Figure 8) so that over the short duration of their simulation (~64 ms) only the effects of the WFS speckles were visible.

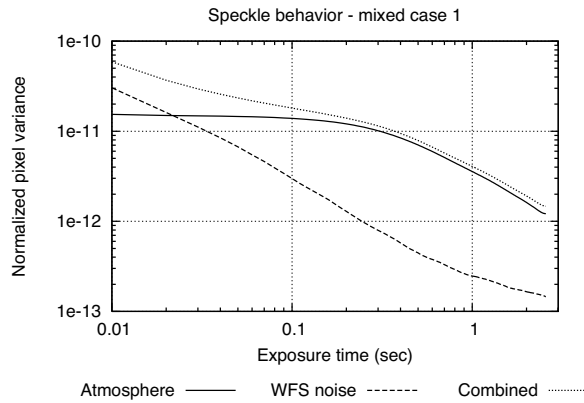


Figure 8: Speckle variance inside the dark hole for a case containing both atmospheric and measurement noise.

4.2 Multiple atmospheric layers

Multiple atmospheric layers complicate the above picture but do not fundamentally modify the long-exposure behavior. Consider two independent phase screens each consisting of a identical sinusoidal phase ripples of frequency \mathbf{k}_0 being translated with respect to each other at velocities \mathbf{v}_1 and \mathbf{v}_2 . When the two are in phase with each other they will interfere constructively, increasing the total power; when they are out of phase by half a period they will interfere destructively and produce a flat wavefront. The total power will oscillate with a period $\mathbf{k}_0 \cdot (\mathbf{v}_1 - \mathbf{v}_2)$. The resulting PSF halo speckle will also oscillate with this period, even in the second-order term. This produces a rapid modulation of the second-order speckles similar to the first-order modulation discussed in section 2. However, the overall speckle evolution will still be set by the atmospheric clearing time D/v_0 where v_0 is the r_0 -weighted average of the velocities of the individual phase screens. Figure 9 illustrates this.

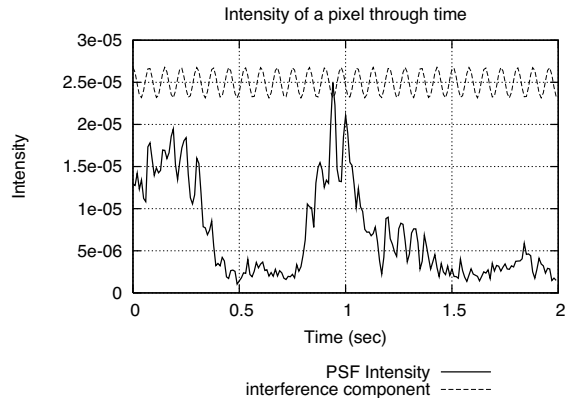


Figure 9: Time series of the intensity of a single pixel in a two-layer atmosphere simulation. The dotted-line interference component shows the expected frequency of the rapid modulation.

5. CONCLUSIONS

The most significant result of our simulations is to show that the decorrelation timescale for residual post-coronagraph PSF speckles caused by atmospheric error sources such as fitting error or temporal bandwidth error is $0.6 D/v$ irrespective of r_0 or the detailed behavior of the AO system; the AO system modifies only the intensity of speckles, not their lifetime. In the absence of a coronagraph the first-order “pinned” speckles are rapidly modulated at a characteristic frequency that depends on field position, but the overall evolution is still dominated by the atmospheric clearing time.

ACKNOWLEDGEMENTS

This research was performed under the auspices of the U.S. Department of Energy by the University of California, Lawrence Livermore National Laboratory under Contract W-7405-ENG-48, and also supported in part by the National Science Foundation Science and Technology Center for Adaptive Optics, managed by the University of California at Santa Cruz under cooperative agreement No. AST – 9876783.

REFERENCES

- ¹ Racine, R., et al. 1999 *PASP* **111**, 587
- ² Marois, C., et al. 2005 *Ap.J.* submitted
- ³ Wallace, J.K., et al. 2004 *Proc. SPIE* **5490**, 370
- ⁴ Angel, J.R.P., 1994, *Nature* **368**, 203
- ⁵ Roddier, F., et al. 1982, *J. Opt. (Paris)*, **13**, 263
- ⁶ Olivier, S.S., et al 1998 in “Brown dwarfs and extrasolar planets”, Rebolo, Martin and Zapatero Osorio eds., ASP Conference Series **134**, 262
- ⁷ Sivaramakrishnan, A., Lloyd, J. P., Hodge, P. E., and Macintosh, B. A. 2002, *Ap.J.* **581**, L59
- ⁸ Perrin, M., et al. 2003 *Ap.J.* **596**, 702
- ⁹ Bloemhof, E., et al. 2001 *Ap.J.* **558**, L71
- ¹⁰ Give’on, A., et al 2005 *Proc. SPIE* **5905**, in press
- ¹¹ Poyneer, L. A. & Macintosh, B. 2004, *JOSA A*, **21**, 810
- ¹² Stahl, S.M., and Sandler, D.G., 1995 *Ap.J.* **454**, L153